Supplementary Information

Synthesis of magnetic mesoporous Fe_3O_4@SB nanocomposite adsorbent for efficient removal of pharmaceutical active compounds from water solution

Somayyeh Shenavaie asl[a], Afshin Pourahmad[a,*], Somayyeh Rostamzadeh Mansour[b], and Nastaran Sohrabi-Gilani[b]

[a]*Department of Chemistry, Ra.C., Islamic Azad University, Rasht, Iran*
[b]*Department of Chemistry, Ard.C., Islamic Azad University, Ardebil, Iran*
* Corresponding author email: *pourahmad@iau.ac.ir*

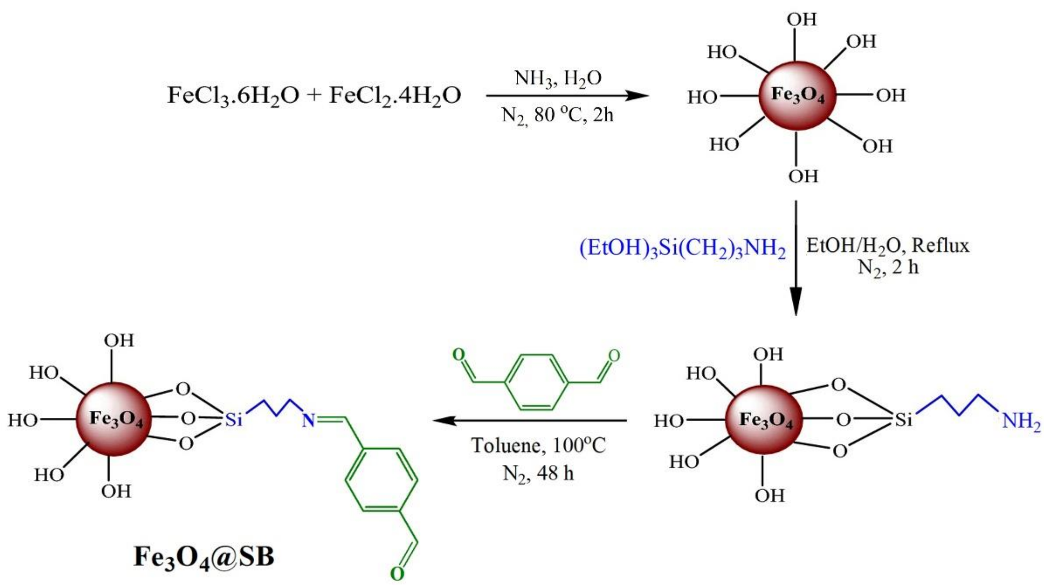

Scheme 1. The synthesis procedure of Fe_3O_4@SB nanocomposite.

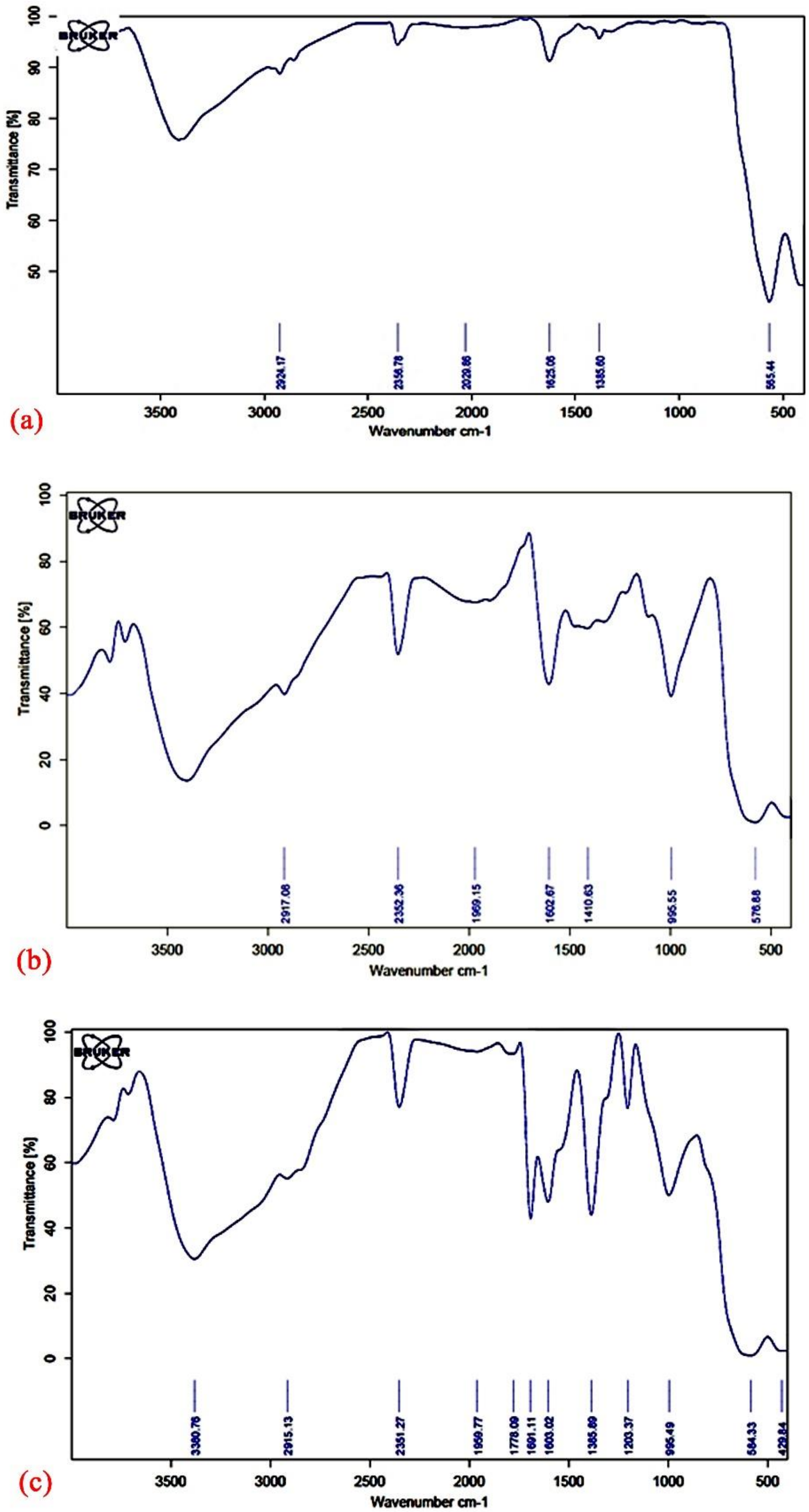

Figure 1. FT-IR spectrum of (a) Fe_3O_4 NPs, (b) Fe_3O_4-APTMS, (c) Fe_3O_4@SB.

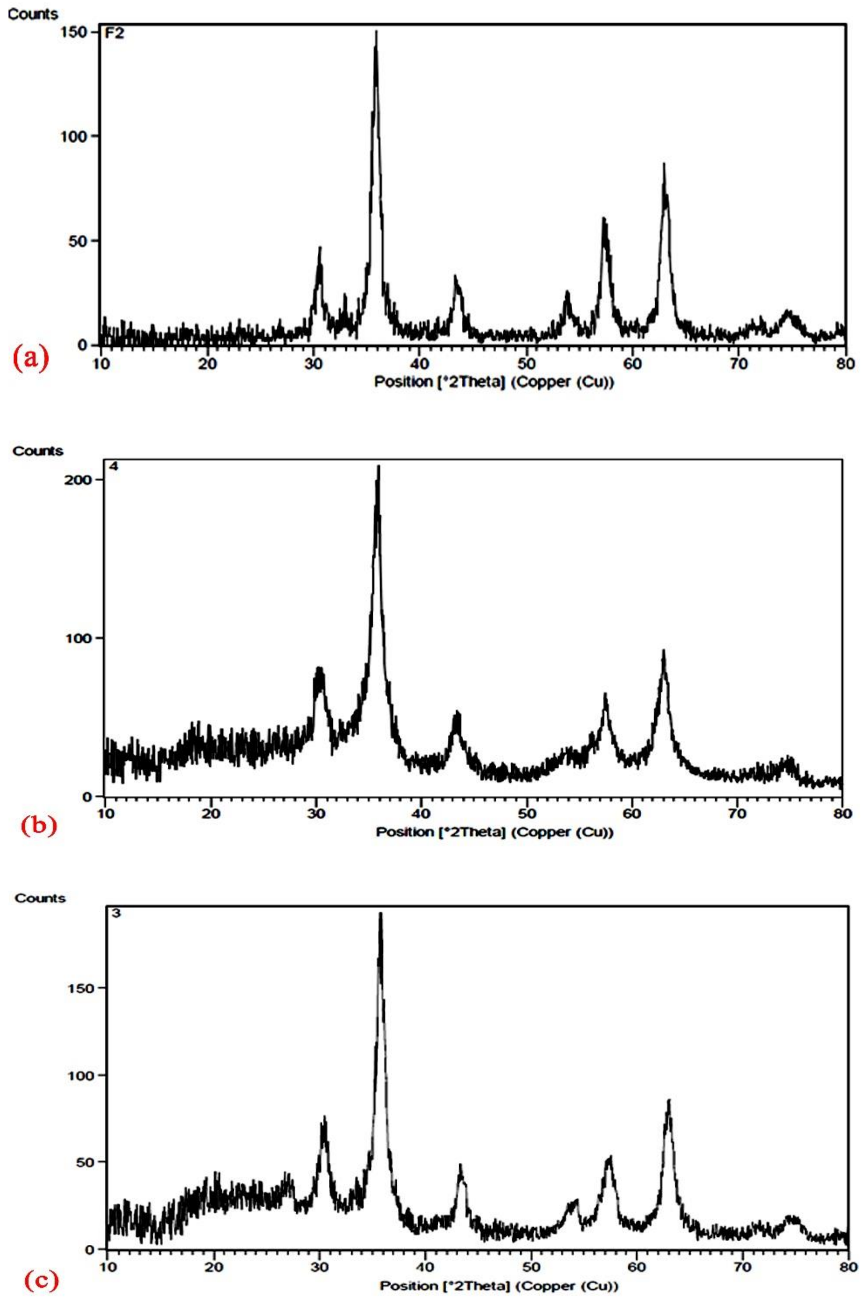

Figure 2. XRD pattern of (a) Fe_3O_4 NPs, (b) Fe_3O_4@NH_2, and (c) Fe_3O_4@SB.

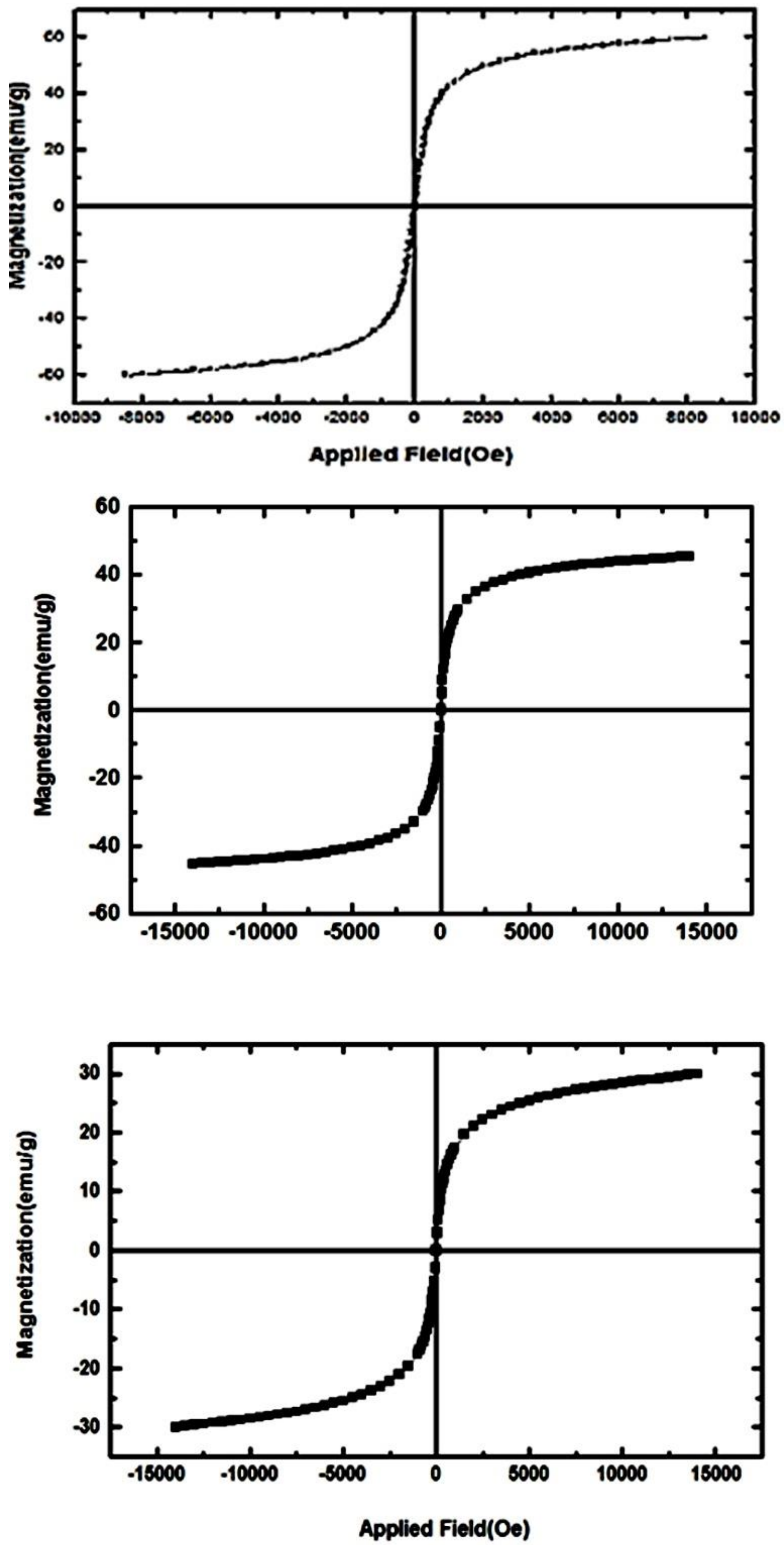

Figure 3. VSM analysis graph of (a) Fe_3O_4 NPs, (b) Fe_3O_4@NH_2, and (c) Fe_3O_4@SB

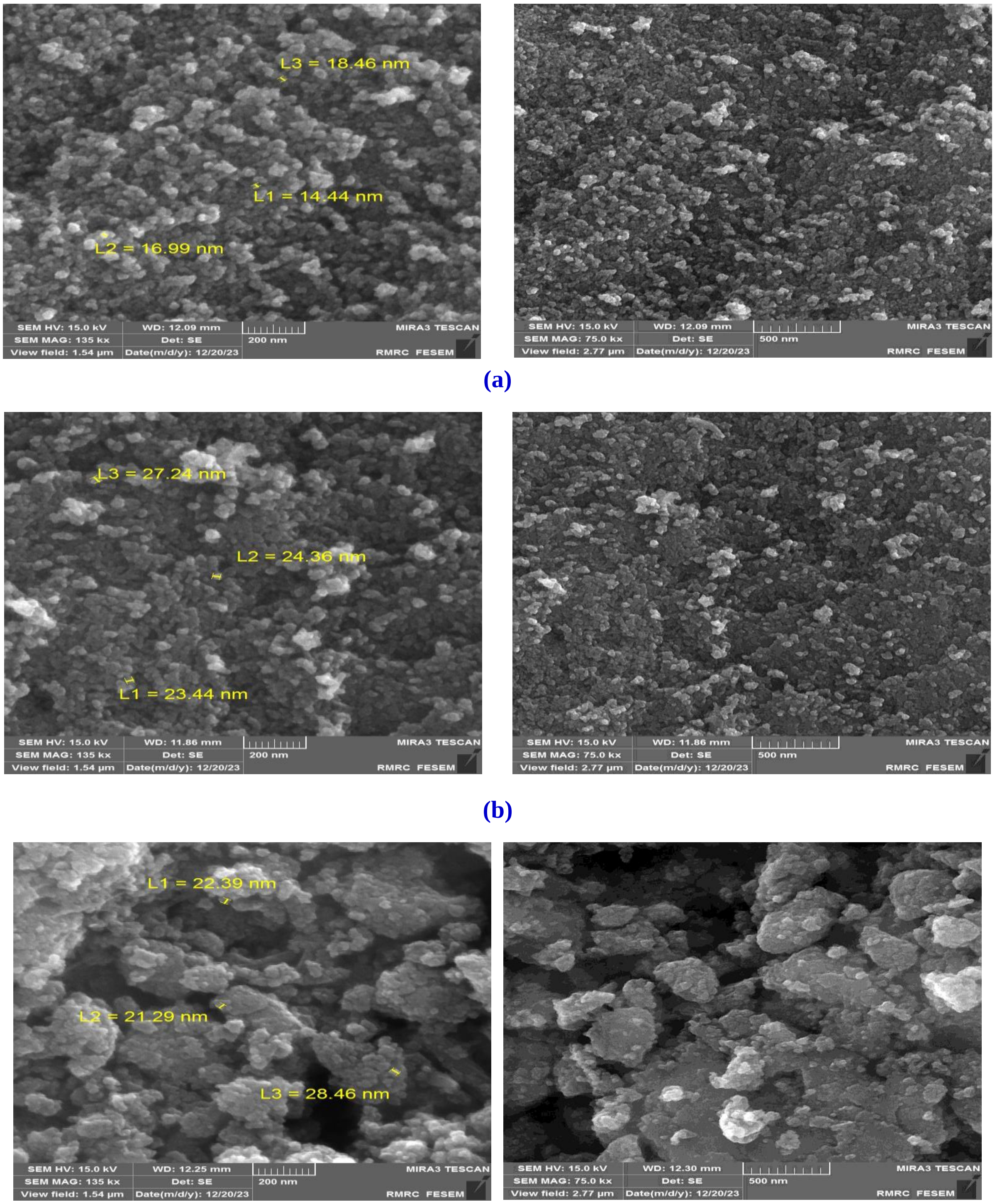

(c)

Figure 4. SEM images of (a) Fe_3O_4 NPs, (b) $Fe_3O_4@NH_2$, and (c) $Fe_3O_4@SB$.

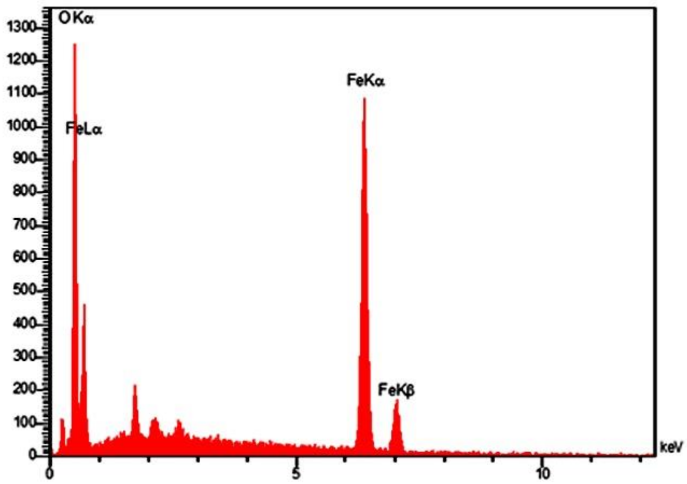

(a)

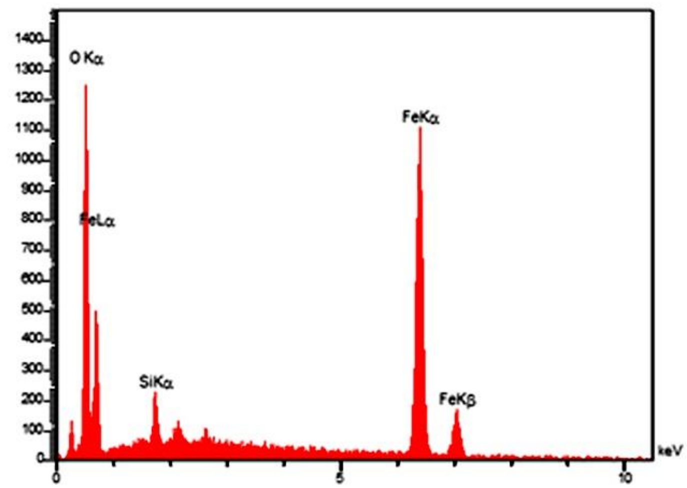

(b)

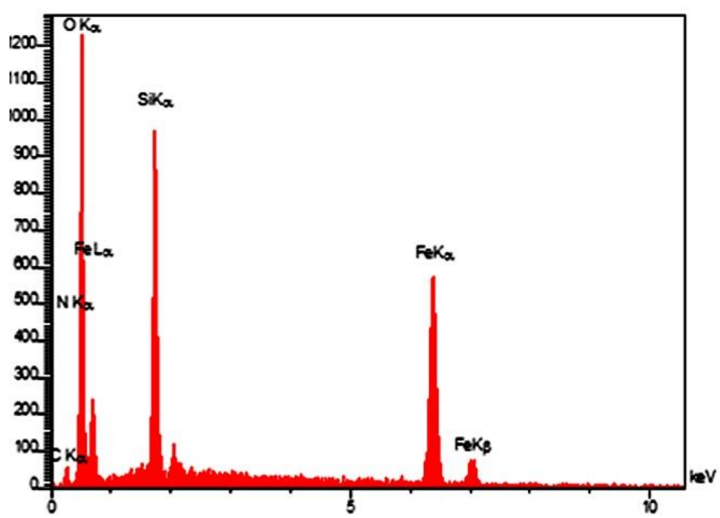

(c)

Figure 5. EDAX analysis of (a) Fe_3O_4 NPs, (b) Fe_3O_4@NH_2, and (c) Fe_3O_4@SB.

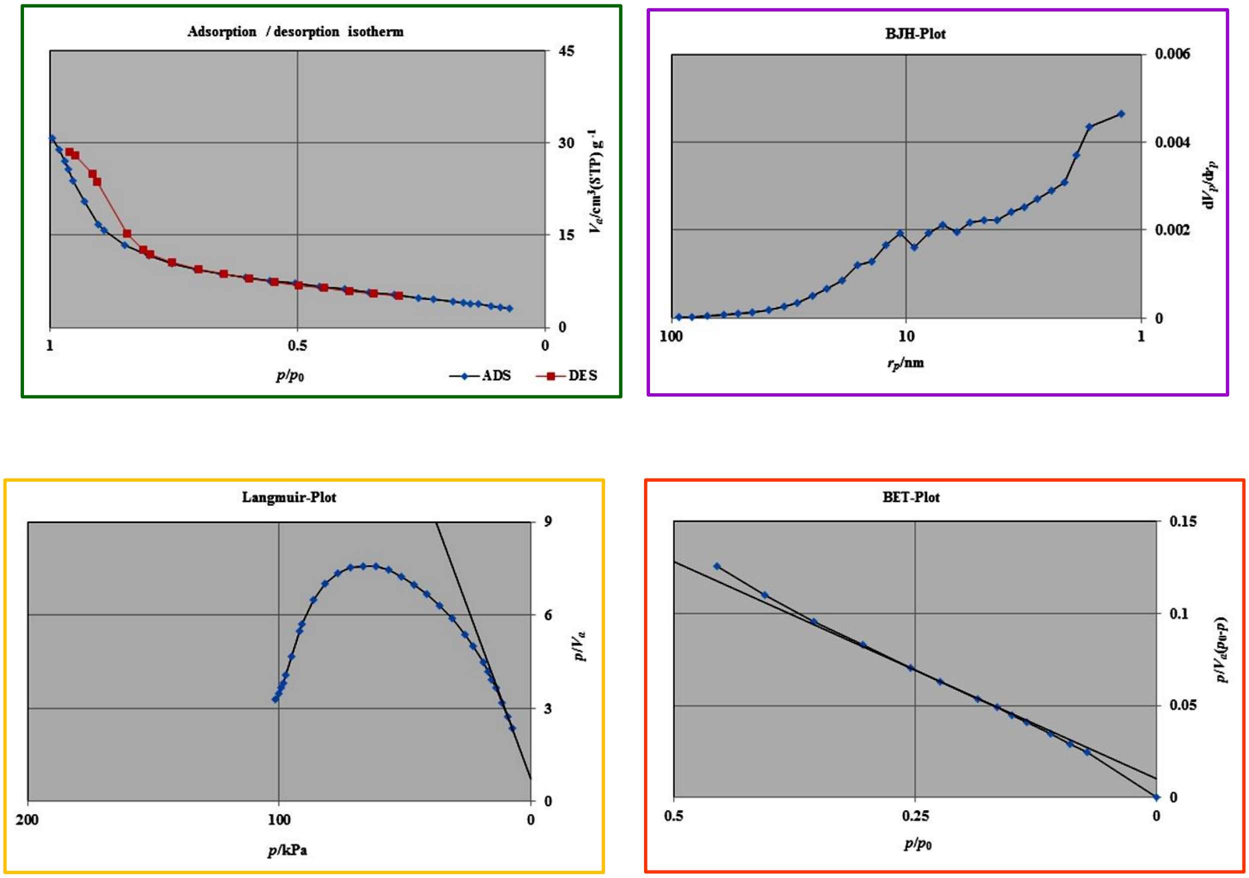

Figure 6. (a) Nitrogen adsorption/desorption isotherm for Fe_3O_4@SB, (b) BJH plot, (c) Langmuir plot, and (d) BET plot

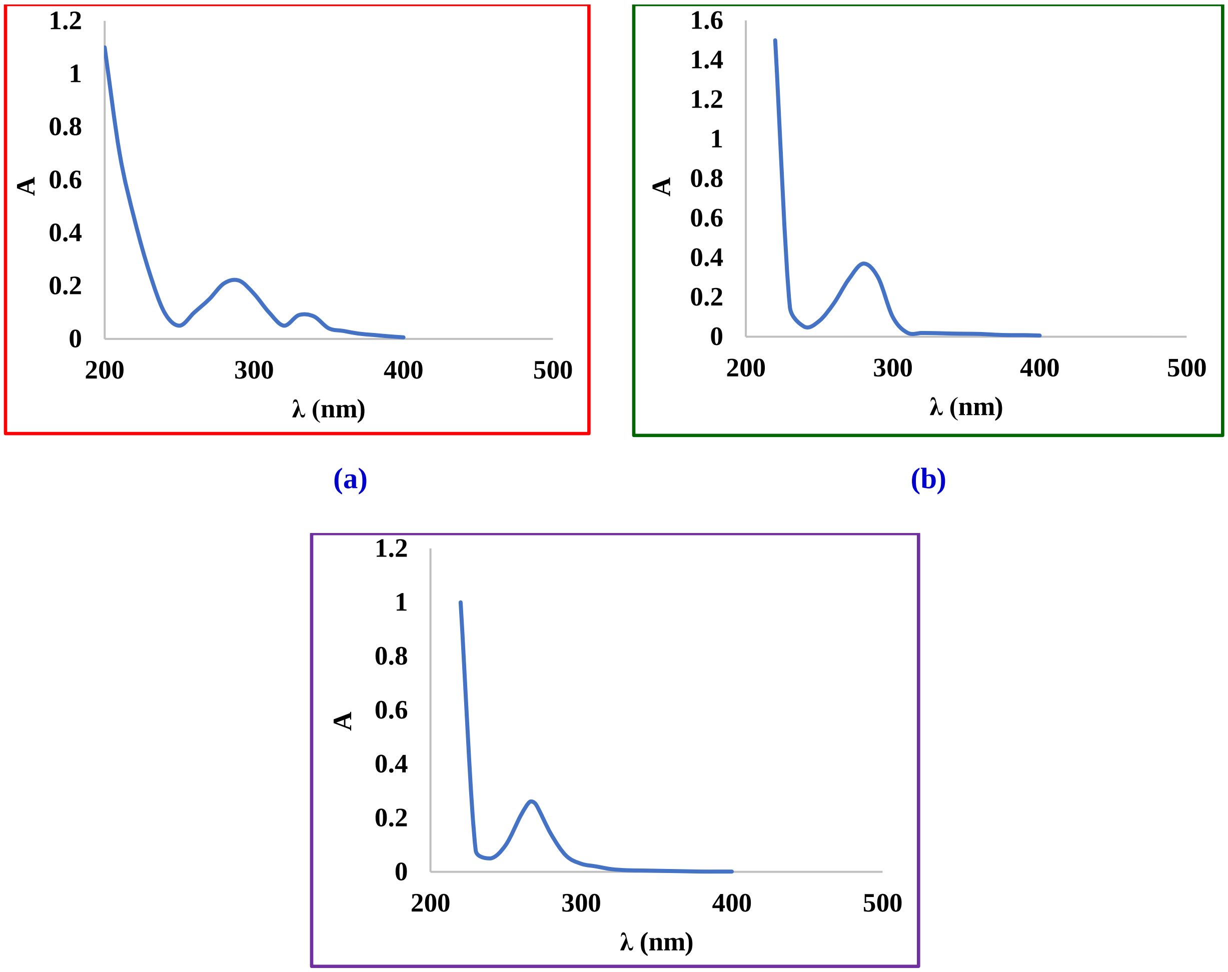

Figure 7. UV/Vis absorption spectra of (a) MA; (b) TRP and (c) 5-FU.

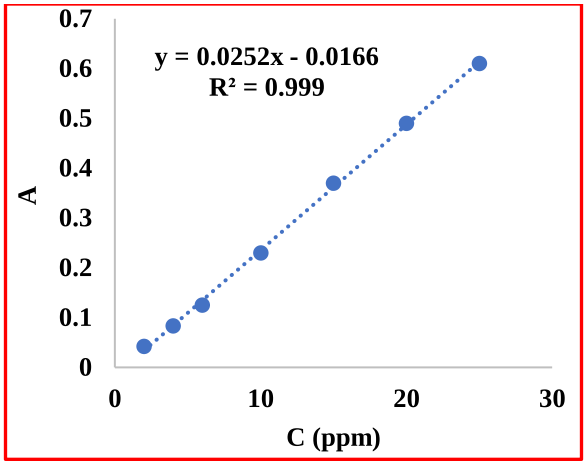

(a)

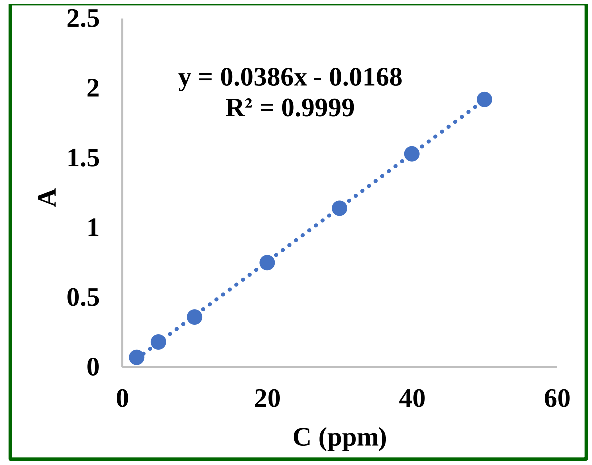

(b)

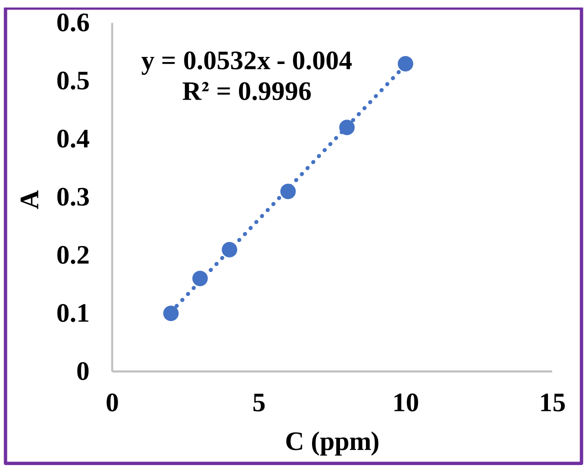

(c)

Figure 8. Calibration curves for (a) MA; (b) TRP; and (c) 5-FU.

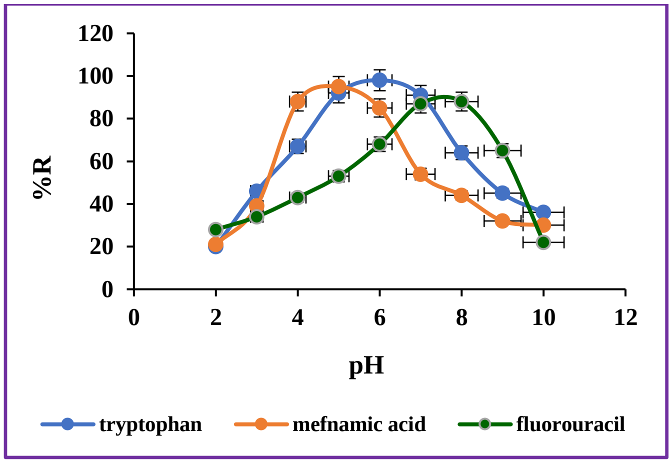

Figure 9. Effect of pH on the removal percentage of PhACs by Fe_3O_4@SB.

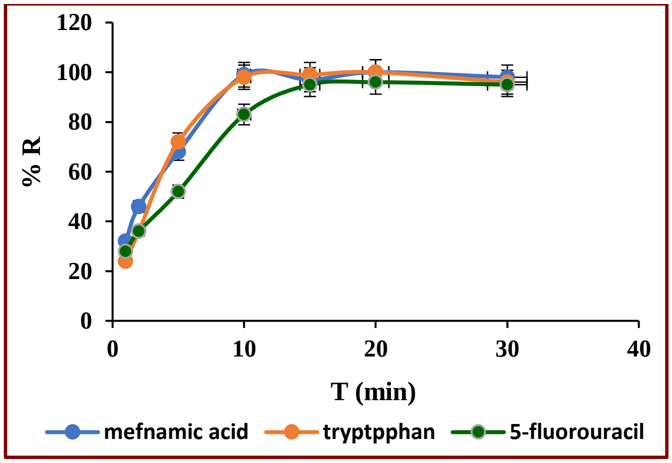

Figure 10. Effect of contact time on the removal percentage of PhACs by Fe_3O_4@SB.

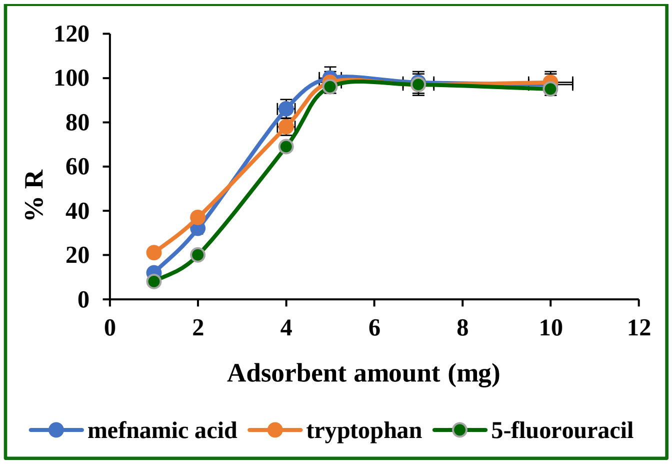

Figure 11. Effect of adsorbent dosage on the removal percentage of PhACs by Fe_3O_4@SB.

Isotherm adsorption chart Langmuir	Isotherm adsorption chart Freundlich

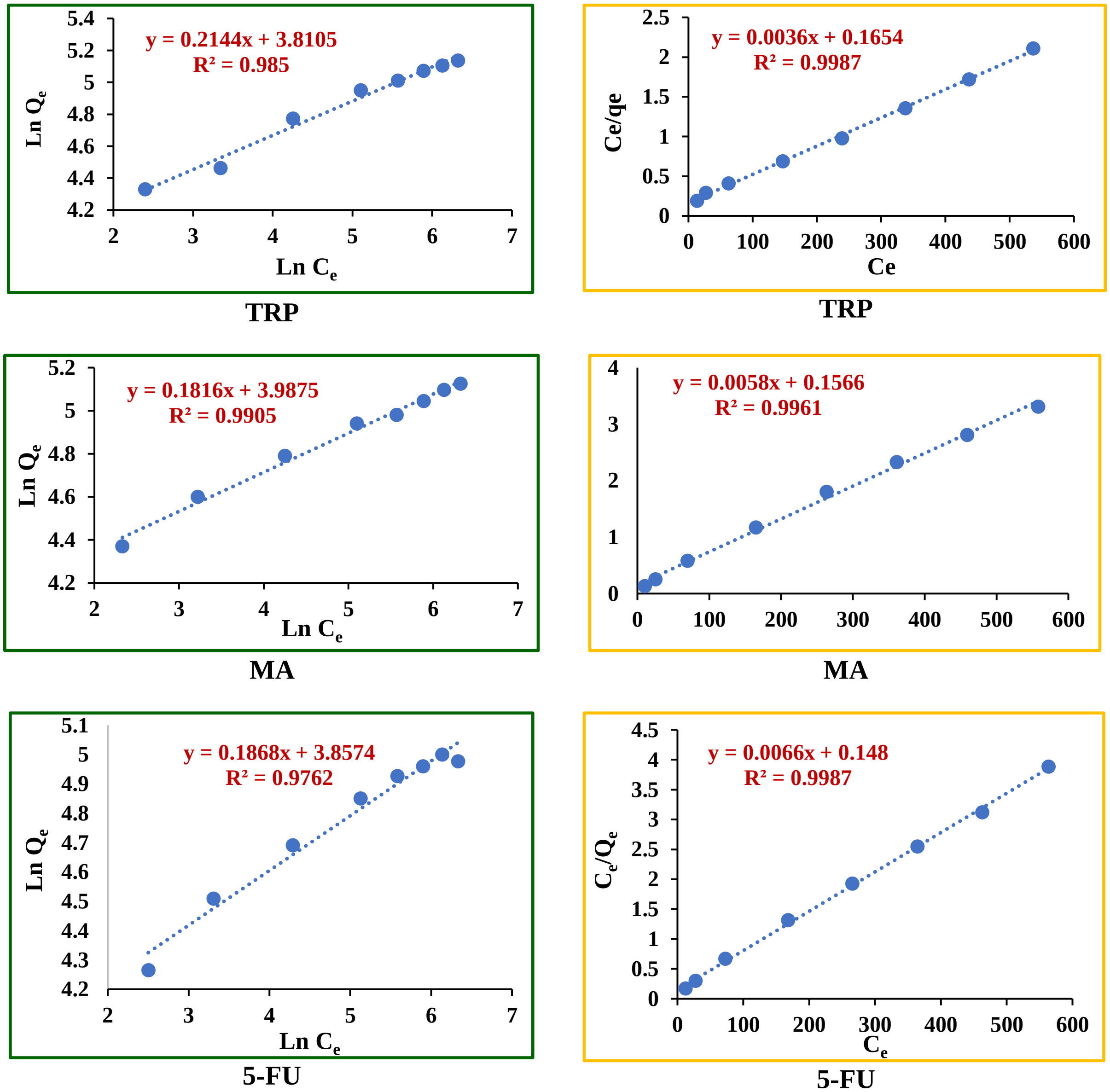

Figures 12. Langmuir and Freundlich adsorption isotherms for PhACs on Fe_3O_4@SB.

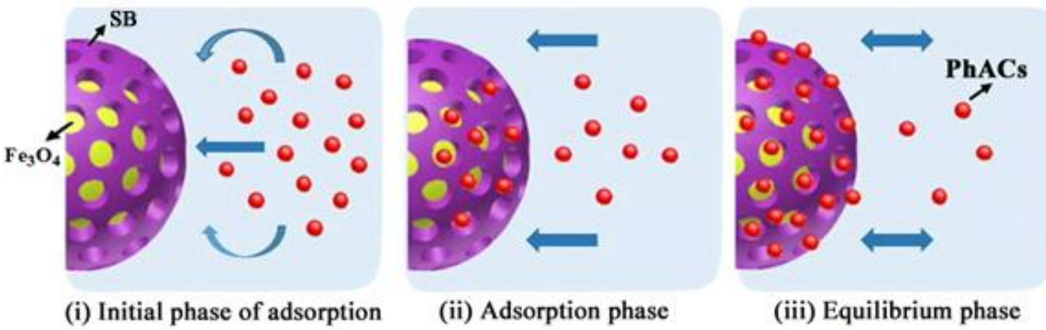

Figure 13. Proposed adsorption mechanisms of PhACs on Fe_3O_4@SB.

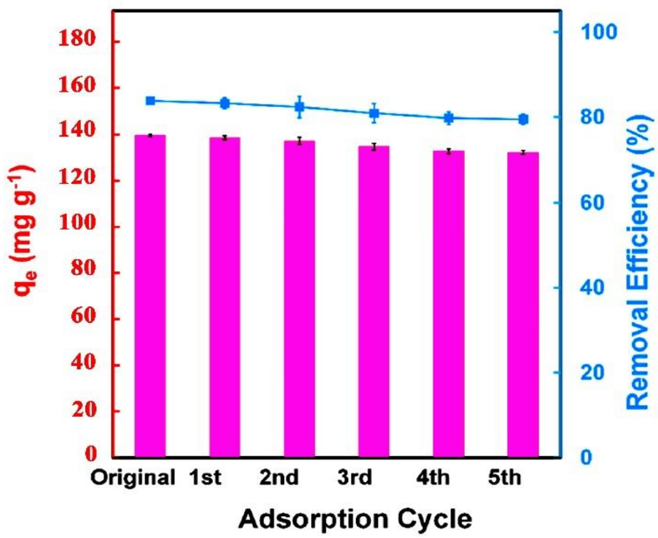

Figure 14. Reusability of the Fe_3O_4@SB nanocomposite.

Table 1. The primary diffraction peaks and the corresponding Miller indices.

2θ (approx., Cu Kα)	Miller Indices (hkl)	Relative Intensity
~18.3°	(111)	Low
~30.1°	(220)	Medium
~35.5°	**(311)**	**Very High**
~37.1°	(222)	Low
~43.1°	(400)	Medium
~53.5°	(422)	Medium
~57.0°	(511)	Medium
~62.6°	(440)	High

Table 2. The Magnetic properties of Fe_3O_4 NPs, Fe_3O_4@NH_2 and Fe_3O_4@SB.

Samples	M_s (emu g^{-1})	H_c (O_e)	M_r (emu g^{-1})
Fe_3O_4	60	0	0
Fe_3O_4@NH_2	42	0	0
Fe_3O_4@SB	30	0	0

Table 3. Removal efficiency of PhACs by Fe_3O_4@SB.

Pharmaceutical compound	pH	Adsorbent dosage (mg)	Contact time (min)	Average removal (%)
Mefenamic acid (MA)	4	5	10	98.07
Tryptophan (TRP)	6	5	10	98.27
5-Fluorouracil (5-FU)	8	5	15	96.53

Table 4. Intraday and interday precision of the adsorption method for PhACs using Fe_3O_4@SB.

Pharmaceutical compound	Concentration (mg L^{-1})	Intraday RSD (%, n=5)	Interday RSD (%, n=5)
Mefenamic acid (MA)	5	1.27	1.23
Tryptophan (TRP)	5	1.85	1.56
5-Fluorouracil (5-FU)	5	2.18	2.02

Table 5. Proposed adsorption mechanisms for PhACs on Fe_3O_4@SB at their respective optimal pH conditions.

Pharmaceutical compound	pH	Dominant species at optimal pH	Interaction mechanism
Mefenamic acid (MA)	4	Molecular ($pK_a \approx 4.2$)	π-π Stacking & hydrogen bonding: The molecular form of MA and the non-protonated imine groups on the adsorbent facilitate strong π-π interactions and hydrogen bonding.
Tryptophan (TRP)	6	Zwitterion (pI = 5.9)	π-π Stacking & hydrogen bonding: The zwitterionic form, with a net neutral charge, maximizes π-π interactions and multi-dentate hydrogen bonding, minimizing electrostatic repulsion.
5-Fluorouracil (5-FU)	8	Molecular ($pK_a \approx 8.0$)	Hydrogen bonding & pore filling: The molecular state preserves the ability of C=O and N-H groups to act as hydrogen bond donors/acceptors. Concurrently, the mesoporous structure allows for efficient physical entrapment.

Table 6. Langmuir and Freundlich adsorption isotherm parameters.

Pharmaceutical compound	Langmuir parameters			Freundlich parameters		
	Q_{max} (mg g^{-1})	K_L (L mg^{-1})	R^2	K_F (L mg^{-1})	1/n	R^2
TRP	175.45	0.032	0.985	45.17	0.210	0.998
MA	172.41	0.037	0.990	53.91	0.181	0.996
5-FU	151.50	0.044	0.976	47.37	0.186	0.998

Table 7. Comparative analysis of adsorption performance for PhACs removal.

Adsorbent material	Target contaminant	Adsorption capacity (mg g^{-1})	Equilibrium time (min)	Optimal pH	Adsorption mechanism(s)	Reference
β-CD-functionalized magnetic clusters	Bisphenol A	52.7	30	7	Host-guest inclusion, H-bonding	[54]
Magnetic activated carbon	Sulfamethoxazole	104.5	1440 (24 h)	6	Pore filling, π-π EDA	[55]
Fe_3O_4/Chitosan/Polypyrrole	Cr(VI)	186.5	120	2	Electrostatic, reduction	[56]
Fe_3O_4@ZIF-67/$CuCo_2S_4$	Ciprofloxacin	400.0	90	6	Complexation, electrostatic	[57]
MIL-101-NH_2(Co/Fe)	5-FU	196.1	120	7	Electrostatic, π-π, H-bonding	[58]
Fe_3O_4@COF (TPA-HMD)	MA	243.9	5	4	Hydrogen bonding, π–π stacking, electrostatic attraction, hydrophobic interactions	[59]
	TRP	277.78	5	6	Hydrogen bonding, π–π stacking, electrostatic, hydrophobic interactions	
	5-FU	208.33	10	8	Hydrogen bonding, pore filling weak π–π stacking	
Fe_3O_4@COF (TAPT-DHTA)	Aflatoxins, Zearalenone	125.8 - 185.2	~5	N/A	Hydrophobic, π-π, size exclusion	[60]
Fe_3O_4@SB	MA	172.41	10	4	π-π stacking, hydrogen bonding	This work
	TRP	175.45	10	6	π-π stacking, hydrogen bonding	
	5-FU	151.50	15	8	Hydrogen bonding, pore filling	

Table S1. Summary of BET results information.

BET plot		
V_m	4.0636	[cm^3(STP) g^{-1}]
$a_{s,BET}$	17.687	[m^2 g^{-1}]
C	24.381	
Total pore volume(p/p_0=0.990)	0.046664	[cm^3 g^{-1}]
Mean pore diameter	10.554	[nm]
Langmuir plot		
Vm	4.5556	[cm^3(STP) g^{-1}]
$a_{s,Lang}$	19.828	[m^2 g^{-1}]
B	0.3035	
BJH plot		
Plot data	Adsorption branch	
V_p	0.04654	[cm^3 g^{-1}]
$r_{p,peak}(Area)$	1.22	[nm]
a_p	17.214	[m2 g-1]

Table S2. Results of optical absorbance measurements for different concentrations of mefenamic acid to construct the calibration graph.

Absorption (A)	Concentration of mefenamic acid(mg L^{-1})
0.042	2
0.083	4
0.125	6
0.23	10
0.37	15
0.49	20
0.61	25

Table S3. Results of optical absorbance measurements for different concentrations of tryptophan to construct the calibration graph.

Absorption (A)	Concentration of tryptophan (mg L^{-1})
0.07	2
0.18	5
0.36	10
0.75	20
1.14	30
1.53	40
1.92	50

Table S4. Results of optical absorbance measurements for different concentrations of 5-fluorouracil to construct the calibration graph.

Absorption (A)	Concentration of 5-fluorouracil (mg L^{-1})
0.10	2
0.16	3
0.21	4
0.31	6
0.42	8
0.53	10